Thermodynamic Aspects and Biological Profile of CDAN/DOPE and DC-Chol/DOPE Lipoplexes[†]

Michael Keller,*[,‡] Michael R. Jorgensen,[‡] Eric Perouzel,[‡] and Andrew D. Miller*[,§]

IC-Vec Ltd., Flowers Building, Armstrong Road, London SW7 2AZ, United Kingdom, and Imperial College Genetic Therapies Centre, Department of Chemistry, Flowers Building, Armstrong Road, Imperial College London, London SW7 2AZ, United Kingdom

Received December 24, 2002; Revised Manuscript Received January 29, 2003

ABSTRACT: The DNA complexation and condensation properties of two established cationic liposome formulations, CDAN/DOPE (50:50, *m*/*m*; Trojene™) and DC-Chol/DOPE (60:40, *m*/*m*), were investigated by using a combination of isothermal titration calorimetry (ITC), circular dichroism (CD), photon correlation spectroscopy (PCS), and turbidity assays. Plasmid DNA (7528 bp) was titrated with extruded liposomes (90 ± 15 nm) and a thermodynamic profile established. ITC data revealed that the two liposome formulations differ substantially in their DNA complexation characteristics. Equilibrium dissociation constants for CDAN/DOPE ($K_d = 19 \pm 3$ μM) and DC-Chol/DOPE liposomes ($K_d = 2 \pm 0.5$ μM) were obtained by fitting the experimental data in a one-site binding model. Both CDAN/DOPE and DC-Chol/DOPE binding events take place with a negative binding enthalpy ($\Delta H° = -0.5$ and -1.7 kcal/mol, respectively) and increasing system entropy ($T\Delta S = 6 \pm 0.3$ and 6.2 ± 0.3 kcal/mol, respectively). Interestingly, CDAN/DOPE liposomes undergo substantial rehydration and protonation prior to complexation with pDNA, which is observed as two discrete exothermic signals during titration. No such biphasic effects are seen with respect to the binding between DC-Chol/DOPE and pDNA that appears to be otherwise instantaneous with no rehydration effects. The rehydration and protonation characteristics of CDAN/DOPE liposomes in comparison with those of DC-Chol/DOPE cationic liposomes are confirmed by ITC; CDAN/DOPE liposomes have strongly exothermic dilution characteristics and DC-Chol/DOPE liposomes only mildly endothermic characteristics. Furthermore, analysis of cationic liposome−pDNA binding by CD spectroscopy reveals that CDAN/DOPE−pDNA lipoplexes are more structurally fluid than DC-Chol/DOPE−pDNA lipoplexes. CDAN/DOPE liposomes induced considerable fluctuation in the DNA structure for at least 60 min, whereas liposomes obtained from DC-Chol/DOPE lack the same effect on the DNA structure. Turbidity studies show that DC-Chol/DOPE lipoplexes exhibit greater resistance to serum than CDAN/DOPE lipoplexes, which showed substantial precipitation after incubation for 100 min with serum. Transfection studies on HeLa and Panc-1 cells reveal that CDAN/DOPE lipoplexes are superior in efficacy to DC-Chol/DOPE lipoplexes. CDAN/DOPE liposomes tend to transfect best in normal growth medium (including 10% serum and antibiotics), whereas DC-Chol/DOPE lipoplexes transfect best under serum free transfection conditions.

Cationic liposomes are widely used as gene delivery systems *in vitro* and increasingly *in vivo*. A variety of cationic liposome formulations are now commercially available, with many of them exhibiting very different formulation and transfection characteristics optimized for specific applications. The differences in transfection efficacy under different experimental conditions and on different cell lines are poorly understood. However, it is clear that the nature of the lipids and their formulation are pivotal factors in the constitution of a successful gene delivery vehicle. Cationic liposomes are now recognized as a potent means of assisting the delivery of genes and other nucleic acids to cells. This holds out hope for the possibility that cationic liposomes could play a major role in the future as a core technology in the emerging field of gene therapy. Numerous cationic lipids have been synthesized and successfully used for *in vitro* and *in vivo* transfection (*1*). Extremely rapid developments in molecular biology are making gene therapy a promising new therapeutic modality (*2*, *3*). As of February 2003, there have been 636 clinical trial protocols logged worldwide. Remarkably, 12.1% of the total clinical trials are nonviral, liposome-based therapies (lipofection) accounting for 17.7% of total patients. This clearly demonstrates the growing interest of the medical research community in nonviral gene delivery systems and, as a result, the urgent need for improved lipids, liposomes, and lipoplexes (*1*, *4*, *5*). For this reason, studies on LD (liposome−DNA) particle formation by biophysical techniques provide an important primary evaluation tool for attempting to understand structure−activity relationships pertinent to cationic liposome- and/or micelle-mediated nucleic acid delivery to cells (*6*). This requires the preliminary evaluation of novel liposome formulations by biophysi-

[†] We thank Mitsubishi Chemical Corp./Mitsubishi-Tokyo Pharmaceuticals for supporting the Imperial College Genetic Therapies Centre.

* To whom correspondence should be addressed. M.K.: e-mail, m.keller@icvec.com. A.D.M.: e-mail, a.miller@imperial.ac.uk; telephone, ++44 (0)20 7594 3150; fax, ++44 (0)20 7594 5803.

[‡] IC-Vec Ltd.

[§] Imperial College London.

10.1021/bi0274219 CCC: $25.00
Published on Web 05/03/2003

cal methods. The formation of LD particles is accompanied by substantial structural reorganization of both nucleic acids and cationic liposomes and/or micelles after initial electrostatic interactions (*7*). However, LD particles are frequently unstable toward fusion and aggregation even in low-ionic strength buffers, a characteristic that must be avoided especially for *in vivo* applications (*8*). Therefore, basic research into the complex formation and stability of these lipoplexes is needed to improve our general understanding of the molecular processes underlying the formation of these supramolecular complexes. Despite intensive investigations by many laboratories into the synthesis of novel cationic lipids (cytofectins), their formulation into cationic liposomes, and generation of LD particles (*1*, *4*, *9*−*23*), this problem has not been solved convincingly without recourse to the development of liposome/mu/DNA (LMD) systems (*24*, *25*). Nevertheless, we and others are still experiencing substantial problems in rendering cationic liposome- and/or micelle-based nonviral vector systems viable *in vivo*, primarily because of the chronic instability of LD and even LMD particles in biological fluids such as serum (*26*).

Hence, as an aid to understanding the problem of LD stability and transfection efficiency, we describe here the results of recent biophysical investigations into cationic liposome−pDNA[1] complexation. The interactions between two well-established cationic liposome formulations, CDAN/DOPE (50:50, *m*/*m*), which is known as Trojene™ (Avanti Polar Lipids Inc.) and DC-Chol/DOPE (60:40, *m*/*m*), and pDNA (7528 bp) are studied by means of biophysical methods. Results provide a framework for understanding why CDAN/DOPE cationic liposomes are exceptionally efficient compared with other synthetic cationic lipid-based systems, including DC-Chol/DOPE liposomes, at mediating the efficient transfection of cells under normal cell growth medium conditions (including 10% serum and antibiotics), allowing for "minimum-handling" transfections. Our data suggest that LD particles prepared from extruded CDAN/DOPE cationic liposomes and pDNA are notably metastable compared with DC-Chol/DOPE-prepared LD particles and others. This metastability may be related to an unusually low amino pK_a value of 5.7 ± 0.01 as measured potentiometrically (*5*).

EXPERIMENTAL PROCEDURES

Synthesis of CDAN. The synthesis of CDAN **9** was conducted in a manner similar to that previously published with a few alterations (Scheme 1) (*1*, *4*, *5*). Briefly, 2-aminoethan-1-ol was Cbz-protected to give **1** and the free alcohol converted to the bromide **2** in 88 and 70% yields, respectively. In a three-step reaction, the bromide was displaced with 3-aminopropan-1-ol, the free alcohol protected with *tert*-butyldiphenylsilyl chloride, and, finally, the secondary amine Cbz-protected, affording, after chromatography, pure **3** (38% overall yield). Next, the alcohol **4** was liberated with TBAF and transformed to the azide **5** via the activated mesylate (72% for three steps).

Scheme 1[a]

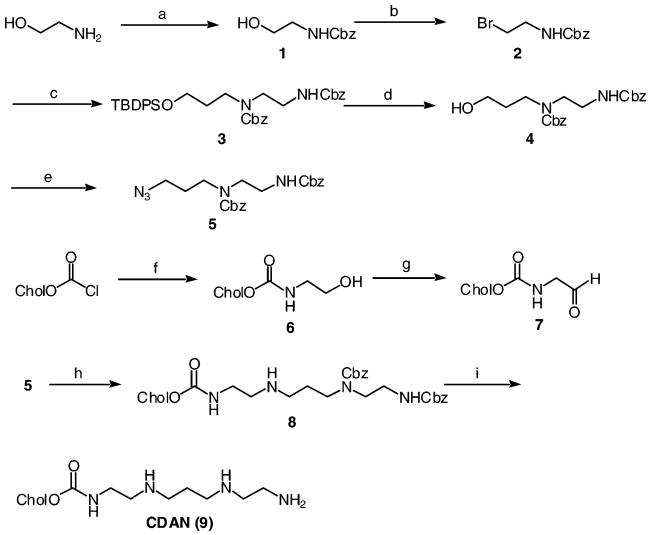

[a] (a) Cbz-Cl, Et_3N, CH_2Cl_2, room temperature, 88%; (b) PPh_3, CBr_4, CH_2Cl_2, room temperature, 70%; (c) (1) 3-aminopropan-1-ol, NaI, K_2CO_3, room temperature, 66%, (2) TBDPS-Cl, Et_3N, DMAP, CH_2Cl_2, room temperature, 84%, (3) Cbz-Cl, Et_3N, room temperature, 69%; (d) TBAF, THF, room temperature, 91%; (e) (1) MsCl, Et_3N, room temperature, 99%, (2) NaN_3, NaI, 80 °C, 80%; (f) 2-aminoethan-1-ol, CH_2Cl_2, room temperature, 88%; (g) Dess−Martin periodinane, CH_2Cl_2, room temperature, 88%; (h) (1) PMe_3, THF, room temperature, (2) THF, room temperature, (3) $NaBH_4$, EtOH, room temperature (64% overall); (i) 10% Pd/C, cyclohexene, EtOH, room temperature, 99%. Abbreviations: CBz-Cl, carbobenzyloxy chloride; TBDPS-Cl, *tert*-butyldiphenylsilyl chloride; TBAF, tetra-*n*-butylammonium fluoride; MsCl, methanesulfonyl chloride (mesyl chloride); Chol-OH, cholesterol.

Cholesteryl alcohol **6** was synthesized from the reaction of cholesterol chloroformate and 2-aminoethan-1-ol in a good 88% yield, followed by oxidation of the primary alcohol with Dess−Martin periodinane to give aldehyde **7** (88% yield). Azide **5** and aldehyde **7** were coupled together in an aza-Wittig type reaction followed by an *in situ* reduction of the resultant imine to afford the partially CBz-protected CDAN **8** (64% yield). Transfer hydrogenolytic deprotection of **8** yielded pure CDAN **9** quantitatively.

General Procedures. ^{1}H NMR spectra were recorded on either Brucker AM 500, Brucker DRX_{400}, Brucker DRX_{300}, or JEOL GX-270Q spectrometers, using a residual isotopic solvent ($CHCl_3$, δ_H = 7.26 ppm) as an internal reference. ^{13}C NMR spectra were also recorded on the same range of spectrometers at 125, 100, 75, and 68.5 Hz, respectively, employing $CDCl_3$ (δ_C = 77.2 ppm) as an internal reference. Infrared spectra were recorded on a Mattson 5000 FTIR spectrometer. Mass spectra were recorded on a Micromass AutoSpecQ mass spectrometer. Elemental combustion analysis was performed at the Imperial College Chemistry Department microanalytical laboratory. Melting points were measured on a Reichert hot stage apparatus and are uncorrected. Chromatography refers to flash column chromatography performed on Merck Kieselgel 60 (230−400 mesh). TLC refers to thin-layer chromatography performed on precoated Merck Kieselgel 60 F_{254} aluminum-supported plates and visualized with ultraviolet light (254 nm), iodine, 4,4′-bis(dimethylamino)benzhydrol in acetone, acidic ammonium molybdate(IV), aqueous potassium manganate(VII), ethanolic vanillin, and acidic methanolic 2,4-dinitrophenylhydrazine, as appropriate. Dichloromethane was distilled

[1] Abbreviations: DC-Chol, 3β-{*N*-[(*N*′,*N*′-dimethylamino)ethane]-carbamoyl}cholesterol; CDAN(B198), *N*^{1}-cholesteryloxycarbonyl-3,7-diazanonane-1,9-diamine; CD, circular dichroism; FCS, fetal calf serum; DOPE, dioleoyl-L-α-phosphatidylethanolamine; HEPES, *N*-(2-hydroxyethyl)piperazine-*N*′-2-ethanesulfonic acid; ITC, isothermal titration calorimetry; pDNA, plasmid DNA; PCS, photon correlation spectroscopy. CDAN/DOPE (50:50, *m*/*m*) is known under its trade name Trojene™ (Avanti Polar Lipids Inc.).

from phosphorus pentoxide. All other dry solvents and chemicals were purchased commercially from Aldrich Chemicals Co. (Dorset, U.K.).

*2-(Benzyloxycarbonyl)aminoethanol (**1**).* To a stirred solution of 2-amino-1-ethanol (22 mL, 360 mmol, 2 equiv) in CH_2Cl_2 (250 mL) at 0 °C was added a solution of carbobenzyloxy chloride (25 mL, 171 mmol) in CH_2Cl_2 (50 mL) over a period of 15 min. After the addition, the reaction mixture was allowed to warm to room temperature and stirred for 4 h. The reaction mixture was poured into saturated aqueous NH_4Cl (120 mL), the organic phase separated, and the aqueous layer extracted with CH_2Cl_2 (2 × 50 mL). The combined organic layers were washed with water (2 × 90 mL) and brine (130 mL) and dried (Na_2SO_4), and the solvent was evaporated under reduced pressure to give after crystallization (CH_2Cl_2/hexanes) 2-(benzyloxycarbonyl)aminoethanol **1** (30 g, 88%) as a colorless, crystalline solid: R_f = 0.16 (ether); mp 63 °C; IR (CH_2Cl_2) ν_{max} 3414, 2949, 1692, 1586, 1533, 1455, 1376, 1259, 1143, 1067 cm^{-1}; ^1H NMR (400 MHz) δ 7.29 (5H, m, Ph), 5.80 (1H, t, J = 5.5 Hz, ZN*H*), 5.05 (2H, s, PhCH_2O), 3.84 (1H, t, J = 5.0 Hz, *H*O), 3.58 (2H, q, J = 5.0 Hz, H-1), 3.24 (2H, dt, J = 5.5 and 5.0 Hz, H-2); ^{13}C NMR (75 MHz) δ 157.23 [NH*C*(O)O], 136.42 (C-1″ of Ph), 128.50−128.02 (rest Ph), 66.77 (Ph*C*H_2), 61.58 (C-1), 43.39 (C-2); HRMS (FAB) *m*/*z* 196 [(M + H)$^+$], 152 [(MH − CO_2)$^+$], 120, 91 [(C_7H_7)$^+$], 77 [(C_6H_5)$^+$], 65, 51; found (M + H)$^+$ 196.0985, calcd for $C_{10}H_{14}NO_3$ (M + H)$^+$ 196.0974. Anal. Found: C, 61.67; H, 6.58; N, 7.13. Calcd for $C_{10}H_{13}NO_3$: C, 61.47; H, 6.71; N, 7.17.

*Preparation of 2-Bromo-N-benzyloxycarbonylethanamine (**2**).* 2-(Benzyloxycarbonyl)aminoethanol **1** (27 g, 150 mmol) in CH_2Cl_2 (250 mL) was treated with CBr_4 (70 g, 211 mmol) and PPh_3 (79 g, 300 mmol) at 0 °C and the resultant mixture stirred at room temperature for 3 h. The reaction was quenched with water (200 mL) and the organic layer collected and washed with water (2 × 200 mL) and brine (200 mL). The organic layer was dried ($MgSO_4$) and the solvent removed under reduced pressure. The resultant solid residue was triturated with warm ether, the mixture then cooled, and the insoluble triphenylphosphine oxide removed by filtration. The filtrate was concentrated and after chromatography (20−100% ether/petrol) gave 2-bromo-*N*-benzyloxycarbonylethanamine **2** (20.2 g, 70%): R_f = 0.63 (ether); IR (CH_2Cl_2) ν_{max} 3415, 3328, 3065, 2960, 1695, 1537, 1455, 1365, 1256, 1179, 1052 cm^{-1}; ^1H NMR (400 MHz) δ 7.33−7.29 (5H, m, Ph), 5.76 (1H, br s, ZN*H*), 5.09 (2H, s, PhCH_2O), 3.50 (2H, m, H-2), 3.37 (2H, t, J = 6.0 Hz, H-1); ^{13}C NMR (75 MHz) δ 156.43 [NH*C*(O)O], 136.40 (C-1″ of Ph), 129.08−128.12 (rest Ph), 66.88 (Ph*C*H_2), 43.25 (C-2), 32.22 (C-1); HRMS (FAB) *m*/*z* 260 [(M[Br^{81}] + H)$^+$], 258 [(M[Br^{79}] + H)$^+$], 150 [(MH − BnOH)$^+$], 121, 105, 91 [(C_7H_7)$^+$], 77 [(C_6H_5)$^+$], 69, 55, 41; found [(M[Br^{79}] + H)$^+$] 258.0133, calcd for $C_{10}H_{13}{}^{79}BrNO_2$ (M[Br^{79}] + H)$^+$ 258.0130.

*3-Aza-6-tert-butyldiphenylsilyloxy-N^{1,3}-di(benzyloxycarbonyl)-1-hexanamine (**3**).* This three-step synthetic procedure began with a mono-N-alkylation on a 120 mmol scale. 2-Bromo-*N*-benzyloxycarbonyl-1-ethanamine **2** (31 g, 120 mmol), 3-amino-1-propanol (46 mL, 600 mmol), NaI (3.6 g, 24 mmol), and K_2CO_3 (33 g, 240 mmol) in DMF (600 mL) were stirred at room temperature for 60 h. The mixture was then concentrated under reduced pressure, dissolved in EtOAc (300 mL), and washed with water (2 × 250 mL) and brine (200 mL). The organic extract was dried ($MgSO_4$) and concentrated *in vacuo* to afford the crude alcohol (20 g, 66%). This crude residue (19 g, 75 mmol) was then dissolved in CH_2Cl_2 (200 mL) and treated dropwise with a mixture of TBDPS-Cl (22 mL, 83 mmol), NEt_3 (21 mL, 150 mmol), and DMAP (0.92 g, 7.5 mmol) in CH_2Cl_2 (100 mL). The solution was stirred at room temperature overnight and then poured into saturated aqueous Na_2CO_3 (250 mL) and the organic layer separated and washed with water and brine, then dried ($MgSO_4$), and concentrated *in vacuo* to afford a crude residue of the O-silylated amino alcohol (31 g, 84%). The final step involved the protection of the secondary amine using carbobenzyloxy chloride as described previously in the synthesis of 2-(benzyloxycarbonyl)aminoethanol **1** on a 63 mmol scale. After purification by chromatography (20−75% ether/petrol), 3-aza-6-*tert*-butyldiphenylsilyloxy-*N*^{1,3}-di(phenylmethoxycarbonyl)-1-hexanamine **3** (27 g, 43 mmol, 69%) was obtained as a viscous, colorless liquid: R_f = 0.35 (50% ether/petrol); IR (film) ν_{max} 3335, 2955, 2931, 2848, 1701, 1525, 1455, 1248, 1137 cm^{-1}; ^1H NMR (400 MHz) δ 7.69 (4H, d, J = 6.5 Hz, H-3″ and H-5″ of Ph_2Si), 7.49−7.34 (16H, m, rest Ph), 5.51 (1H, br s, ZN*H*), 5.14−5.10 (4H, m, PhCH_2O), 3.70 (2H, m, H-6), 3.47−3.44 (6H, m, H-1, H-2, H-4), 1.80 (2H, m, H-5), 1.10 (9H, s, Me of *t*-Bu); ^{13}C NMR (75 MHz) δ 157.46 and 157.17 [NH*C*(O)O], 137.15−127.98 (Ph), 67.70 and 67.04 (Ph*C*H_2), 61.93 (C-6), 47.71 (C-4), 45.49 (C-2), 40.51 (C-1), 32.16 (C-5), 27.43 (Me of *t*-Bu), 19.71 (Me_3C); HRMS (FAB) *m*/*z* 625 [(M + H)$^+$], 581 [(MH − CO_2)$^+$], 567 (MH − *t*-Bu), 547 [(M − C_6H_5)$^+$], 491, 305, 268, 197, 135, 91 [(C_7H_7)$^+$], 77 [(C_6H_5)$^+$]; found (M + H)$^+$ 625.3094, calcd for $C_{37}H_{45}N_2O_5Si$ (M + H)$^+$ 625.3098.

*6-Amino-4-aza-N^{4,6}-di(phenylmethoxycarbonyl)-1-hexanol (**4**).* To a solution of 3-aza-6-*tert*-butyldiphenylsilyloxy-*N*^{1,3}-di(phenylmethoxycarbonyl)-1-hexanamine **3** (27 g, 43 mmol) in THF (300 mL) was added TBAF (48 mL of a 1.0 M solution in THF, 47 mmol, 1.1 equiv), and the mixture was stirred for 3 h at room temperature. The reaction was quenched with saturated aqueous $NaHCO_3$ (200 mL) and the THF then removed *in vacuo*. The resulting biphasic oil was diluted with ether (200 mL) and poured into water (150 mL). The aqueous layer was washed with ether (2 × 150 mL), and the organic layers were combined, washed with water (2 × 150 mL) and brine (150 mL), and dried (Na_2SO_4). The solvent was then removed under reduced pressure to give a pale yellow oil, which after chromatography (ether/5−20% acetone), gave 6-amino-4-aza-*N*^{4,6}-di(phenylmethoxycarbonyl)-1-hexanol **4** (15.2 g, 39 mmol, 91%) as a viscous, colorless oil: R_f = 0.41 (75% ether/acetone); IR (CH_2Cl_2) ν_{max} 3646−3396, 3054, 2950, 1679, 1670, 1519, 1452, 1247, 1139 cm^{-1}; ^1H NMR (400 MHz) δ 7.36−7.32 (10H, m, Ph), 5.68−5.41 (1H, br m, ZN*H*), 5.14−5.09 (4H, m, PhCH_2O), 3.58 (2H, m, H-1), 3.45−3.39 (6H, m, H-3, H-5, H-6), 2.70−2.59 (1H, br s, O*H*), 1.70 (2H, m, H-2); ^{13}C NMR (75 MHz) δ 157.10 and 156.77 [NH*C*(O)O], 136.45 and 136.30 (C-1″ of Ph), 128.57−127.92 (rest Ph), 67.56 ($PhCH_2$), 67.32 ($PhCH_2$), 66.68 ($PhCH_2$), 59.50 (C-1), 47.00 (C-5), 44.38 (C-3), 39.73 (C-6), 30.56 (C-2); HRMS (FAB) *m*/*z* 387 [(M + H)$^+$], 343 [(MH − CO_2)$^+$], 279, 242, 167, 150, 133, 120, 105, 91 [(C_7H_7)$^+$], 77 [(C_6H_5)$^+$], 69, 55, 41; found (M + H)$^+$ 387.1914, calcd for $C_{21}H_{27}N_2O_5$ (M + H)$^+$ 387.1920.

*3-Aza-6-azido-$N^{1,3}$-di(phenylmethoxycarbonyl)-1-hexanamine (**5**).* The product was prepared according to a two-step procedure. First, 6-amino-4-aza-$N^{4,6}$-di(phenylmethoxycarbonyl)-1-hexanol **4** (15.2 g, 39 mmol) was mesylated with mesyl chloride and Et_3N (16.4 mL, 118 mmol) in CH_2Cl_2 (150 mL) which after standard workup gave the crude mesylate (18.2 g, 39.2 mmol, 99%) as a pale gum which was used without further purification in the next step. Thus, the mesylate (18.2 g, 39.2 mmol) in DMF (250 mL) was treated with NaI (6.2 g, 41 mmol) and NaN_3 (12.6 g, 194 mmol) and the resultant mixture heated under an N_2 atmosphere at 80 °C for 3 h. The cooled solution was then concentrated *in vacuo*, redissolved in CH_2Cl_2 (150 mL), washed with water (2 × 100 mL) and brine (100 mL), dried ($MgSO_4$), and concentrated *in vacuo* to afford a crude residue. The crude product was chromatographed (ether/hexanes) to afford 6-azido-$N^{1,3}$-di(phenylmethoxycarbonyl)-1-hexanamine **5** (13 g, 80%) as a pure colorless liquid: R_f = 0.64 (75% ether/acetone); IR (film) ν_{max} 3355, 2931, 2096, 1651, 1524, 1455, 1247, 1139 cm^{-1}; ^1H NMR (300 MHz) δ 7.35 (10H, m, Ph), 5.60 (1H, br s, ZN*H*), 5.13−5.09 (4H, m, PhCH_2O), 3.38−3.25 (8H, m, H-1, H-2, H-4, H-6), 1.81 (2H, m, H-5); ^{13}C NMR (75 MHz) δ 156.65 [NH*C*(O)O], 136.48 (C-1″ of Ph), 128.61−127.96 (rest Ph), 67.42 and 66.69 (Ph*C*H_2), 48.85 (C-6), 47.26 (C-2), 45.27 (C-4), 39.88 (C-1), 28.02 (C-5); HRMS (FAB) *m/z* 412 [$(M + H)^+$], 368 [$(MH - CO_2)^+$], 165, 152, 120, 105, 91 [$(C_7H_7)^+$], 77 [$(C_6H_5)^+$], 69, 51; found $(M + H)^+$ 412.2004, calcd for $C_{21}H_{26}N_5O_4$ $(M + H)^+$ 412.1998.

*2-(Cholesteryloxycarbonyl)aminoethanal (**7**).* 2-(Cholesteryloxycarbonyl)aminoethanol **6** (*27*) (2.5 g, 5.3 mmol) in CH_2Cl_2 (200 mL) was treated with Dess−Martin periodinane (3 g, 7 mmol) and the mixture stirred at room temperature for 1.5 h. Pyridine (2.8 mL, 5 equiv) and silica gel (12 g) were added to the solution, and the solvent was removed *in vacuo*. The resultant powder was immediately applied to the top of a pre-prepared flash chromatography column and the column eluted quickly with 2.5% acetone in CH_2Cl_2 to afford the pure 2-(cholesteryloxycarbonyl)aminoethanal **7** (2.0 g, 47 mmol, 88%): R_f = 0.32 (ether); IR (CH_2Cl_2) ν_{max} 3356, 2937, 2868, 1699, 1537, 1467, 1378, 1265, 1137 cm^{-1}; ^1H NMR (300 MHz) δ 9.66 (1H, s, C*H*O), 5.38 (2H, m, ChOCN*H* and H-6′), 4.50 (1H, m, H-3′), 4.13 (2H, d, J = 4.5 Hz, H-2), 2.36−2.18 (2H, m, H-4′), 2.04−1.78 (5H, m, H-2′, H-7′, H-8′), 1.60−1.07 (21H, m, H-1′, H-9′, H-11′, H-12′, H-14′−H-17′, H-20′, H-22′−H-25′), 1.03 (3H, s, H-19′), 0.92 (3H, d, J = 6.5 Hz, H-21′), 0.88 (3H, d, J = 6.5 Hz, H-26′), 0.87 (3H, d, J = 6.5 Hz, H-27′), 0.69 (3H, s, H-18′); ^{13}C NMR (75 MHz) δ 196.85 (*C*HO), 156.00 [NH*C*(O)O], 139.64 (C-5′), 122.68 (C-6′), 75.12 (C-3′), 56.71 (C-14′), 56.18 (C-17′), 51.62 (C-2), 50.02 (C-9′), 42.33 (C-4′), 39.76 (C-16′), 39.54 (C-24′), 36.56 (C-1′), 36.21 (C-22′), 35.82 (C-20′), 31.89 (C-8′), 28.25 (C-12′), 28.03 (C-25′), 24.31 (C-15′), 23.87 (C-23′), 22.84 (C-26′), 22.59 (C-27′), 21.07 (C-11′), 19.35 (C-19′), 18.74 (C-21′), 11.88 (C-18′); HRMS (FAB) *m/z* 369 [(Chol)$^+$], 230, 159, 145, 119, 105, 95 [$(C_7H_{11})^+$], 81 [$(C_6H_9)^+$], 69, 55. Anal. Found: C, 76.49; H, 10.27; N, 2.87. Calcd for $C_{30}H_{49}NO_3$: C, 76.37; H, 10.48; N, 2.97.

*N^1-Cholesteryloxycarbonyl-3,7-diaza-$N^{7,9}$-di(phenylmethoxycarbonyl)-1,9-nonanediamine (**8**).* A solution of 6-azido-$N^{1,3}$-di(phenylmethoxycarbonyl)-1-hexanamine **5** (1.0 g, 2.43 mmol) in THF (8 + 2 mL wash) was transferred under nitrogen to a flask charged with flame-dried 4 Å molecular sieves (4.5 g, 500 mg/mmol) via cannula. To this suspension was added dropwise trimethylphosphine (2.82 mL of a 1.0 M solution in THF, 2.82 mmol, 1.15 equiv) over a period of 5 min. After 45 min, pure 2-(cholesteryloxycarbonyl)-aminoethanal **8** (1.38 g, 2.91 mmol, 2 equiv) in THF (10 + 2 mL wash) was added via cannula. The reaction mixture was stirred for a further 5 h and then the THF concentrated under nitrogen to give a viscous suspension. To this was added ethanol (10 mL) followed by $NaBH_4$ (9.80 mL of a 0.5 M solution in diglyme, 4.90 mmol, 2 molar equiv). Slight effervescence ensued, and the reaction mixture was stirred for a further 24 h. The suspension was filtered through a short bed of Celite and the filter cake washed carefully with CH_2Cl_2 (30 mL). The solvents were then removed under reduced pressure to give a pale yellow oil. This was then diluted with CH_2Cl_2 (50 mL) and poured carefully into saturated aqueous $NaHCO_3$ (60 mL) and the effervescence allowed to cease. The aqueous layer was further washed with CH_2Cl_2 (2 × 15 mL), and the combined organic layers were washed with water (2 × 40 mL) and brine (60 mL) and dried ($MgSO_4$). The solvent was then removed *in vacuo* to give a viscous oil, which after chromatography (96% CH_2Cl_2, 3.5% methanol, and 0.5% NH_3 to 92% CH_2Cl_2, 7% methanol, and 1% NH_3) gave N^1-cholesteryloxycarbonyl-3,7-diaza-$N^{7,9}$-di(phenylmethoxycarbonyl)-1,9-nonanediamine **8** (1.3 g, 64%) as a colorless, sticky solid: R_f = 0.29 (92% CH_2Cl_2/7% methanol/1% NH_3); IR (CH_2Cl_2) ν_{max} 3423−3311, 3035, 2956, 2867, 1718, 1700, 1681, 1526, 1467, 1378, 1139 cm^{-1}; ^1H NMR (300 MHz) δ 7.32 (10H, m, Ph), 5.70−5.50 (2H, br m, ChOCN*H* and ZN*H*), 5.35 (1H, m, H-6′), 5.10−5.07 (4H, m, PhCH_2O), 4.47 (1H, m, H-3′), 3.34−3.16 (8H, m, H-1, H-6, H-8, H-9), 2.65−2.50 (4H, m, H-2 and H-4), 2.33−2.18 (2H, m, H-4′), 2.03−1.81 (5H, m, H-2′, H-7′, H-8′), 1.69−1.08 (24H, m, H-3, H-5, H-1′, H-9′, H-11′, H-12′, H-14′−H-17′, H-20′, H-22′−H-25′), 0.99 (3H, s, H-19′), 0.92 (3H, d, J = 6.5 Hz, H-21′), 0.88 (3H, d, J = 6.5 Hz, H-26′), 0.87 (3H, d, J = 6.5 Hz, H-27′), 0.68 (3H, s, H-18′); ^{13}C NMR (75 MHz) δ 156.45 [NH*C*(O)O], 139.87 (C-5′), 136.54 (C-1″ of Ph), 128.56−127.94 (rest Ph), 122.44 (C-6′), 74.29 (C-3′), 67.35 (Ph*C*H_2), 56.71 (C-14′), 56.20 (C-17′), 50.04 (C-9′), 49.01 (C-2), 47.48−46.66 (C-1, C-6, C-8, C-9), 45.74 (C-4), 42.34 (C-13′), 39.78 (C-4′), 39.55 (C-12′), 38.64 (C-24′), 36.56 (C-1′), 36.23 (C-22′), 35.82 (C-20′), 31.90 (C-8′ and C-7′ overlapping), 28.25 (C-12′), 28.02 (C-16′), 27.1 (C-5), 24.31 (C-15′), 23.88 (C-23′), 22.86 (C-26′), 22.61 (C-27′), 21.08 (C-11′), 19.35 (C-19′), 18.77 (C-21′), 11.90 (C-18′); HRMS (FAB) *m/z* 841 [$(M + H)^+$], 398, 369 [(Chol)$^+$], 161, 133, 121, 105, 91 [$(C_7H_7)^+$], 69, 55, 43; found $(M + H)^+$ 841.5884, calcd for $C_{51}H_{77}N_4O_6$ $(M + H)^+$ 841.5843.

*Preparation of N^1-Cholesteryloxycarbonyl-3,7-diaza-1,9-nonanediamine (CDAN, **9**).* A flask containing N^1-cholesteryloxycarbonyl-3,7-diaza-$N^{7,9}$-di(phenylmethoxycarbonyl)-1,9-nonanediamine **8** (1.3 g, 1.5 mmol) was thoroughly flushed with nitrogen before 10% palladium on charcoal (1.41 g, 1.33 mmol, 0.25 equiv) was added. The mixture was purged again with nitrogen, and ethanol (45 mL) was slowly added with stirring. To this suspension was added cyclohexene (1.5 mL, 15 mmol, 10 equiv), and the mixture was gently refluxed for 1.5 h. The solution was allowed to

cool to room temperature and filtered through a pad of Celite, and the filter cake was washed several times with portions of ethanol (4 × 5 mL). The volatile components were removed under reduced pressure, giving a waxy solid which on prolonged drying under high vacuum gave N^1-cholesteryloxycarbonyl-3,7-diaza-1,9-nonanediamine **9** (850 mg, 99%) as a hygroscopic solid: IR (CH_2Cl_2) ν_{max} 3584−3245, 2937, 2868, 1695, 1538, 1469, 1379, 1251, 1133, 1014 cm^{-1}; ^1H NMR (400 MHz) δ 5.82 (1H, br s, ChOCN*H*), 5.23 (1H, m, H-6′), 4.33 (1H, m, H-3′), 3.54−2.55 (16H, m, H-1−H-4, H-6−H-9, H_2N), 2.21−2.09 (2H, m, H-4′), 1.97−1.73 (5H, m, H-2′, H-7′, H-8′), 1.55−0.99 (23H, m, H-5, H-1′, H-9′, H-11′, H-12′, H-14′−H-17′, H-20′, H-22′−H-25′), 0.88 (3H, s, H-19′), 0.78 (3H, d, J = 6.0 Hz, H-21′), 0.74 (6H, d, J = 6.5 Hz, H-26′ and H-27′), 0.55 (3H, s, H-18′); ^{13}C NMR (100 MHz) δ 156.38 [NH*C*(O)O], 139.70 (C-5′), 122.30 (C-6′), 73.99 (C-3′), 56.56 (C-14′), 56.05 (C-17′), 51.91 (C-4), 49.88 (C-9′), 49.05 (C-6), 48.15 (C-8), 47.95 (C-2), 43.50 (C-9), 42.18 (C-13′), 41.12 (C-1), 39.63 (C-4′), 39.40 (C-12′), 38.53 (C-24′), 36.90 (C-1′), 36.42 (C-10′), 36.08 (C-22′), 35.69 (C-20′), 31.75 (C-8′ and C-7′ overlapping), 29.62 (C-5), 28.12 (C-12′), 27.86 (C-16′), 27.86 (C-2′), 27.86 (C-25′), 24.17 (C-15′), 23.75 (C-23′), 22.73 (C-26′), 22.48 (C-27′), 20.94 (C-11′), 19.24 (C-19′), 18.62 (C-21′), 11.76 (C-18′); HRMS (FAB) *m*/*z* 573 [(M + H)$^+$], 544, 513, 369 [(Chol)$^+$], 215, 175, 147, 121, 95 [(C_7H_{11})$^+$], 69, 55; found (M + H)$^+$ 573.5139, calcd for $C_{35}H_{65}N_4O_2$ (M + H)$^+$ 573.5108.

DNA. Plasmid DNA pUMVC1 (pDNA, 7528 bp) was obtained from the University of Michigan Vector Core (Ann Arbor, MI) (http://www.med.umich.edu/vcore/Plasmids/), amplified, and purified by Bayou Biolabs. The concentration of pDNA was determined spectrophotometrically (A_{260} = 1 ≅ 50 μg/mL), and the pDNA molar concentration was determined using an average nucleotide base pair molecular mass of 660 Da (*28*).

Liposomes. Liposomes were prepared at a concentration of 5 mg of lipid/mL by reversed phase methodology followed by extrusion. For this purpose, 141 μL of DOPE (20 mg/mL) and 217 μL of CDAN (10 mg/mL) or 251 μL of DC-Chol (10 mg/mL) were pipetted into a round-bottomed flask (50 mL), 1 mL of 4 mM HEPES (pH 7.0) was added, and the organic layer was slowly removed under reduced pressure. After removal of all solvent, the pH was adjusted to 7.0 by the addition of concentrated hydrochloric acid (typically 15−20 μL) and the volume adjusted to 1 mL by addition of distilled water. The liposomes were extruded 10 times through 0.1 μm membranes (Millipore, Dublin, Ireland) and their sizes measured by PCS. Both liposome formulations measured 90 ± 15 nm with a polydispersity index of ≈0.

Isothermal Titration Calorimetry Experiments. Binding studies were performed by isothermal titration calorimetry (ITC) using a VP-ITC MicroCalorimeter from MicroCal (Northampton, MA). Titration data were processed by means of the Origin software provided by the manufacturer. Baseline corrections were used for the endothermic aggregation phases to permit the fitting of data points to a single-affinity binding model. Plasmid DNA (24.1 or 18.1 nM) was maintained in the thermostated cell (1.428 mL) at 25 °C in 4 mM HEPES (pH 7.0), and the whole solution was stirred at 350 rpm. Liposomes were introduced into the stirred cell by means of a syringe in one injection of 1 μL, followed by 24 (12 μL) individual injections [each injection containing liposomes (1.92 or 3.84 mM) in 4 mM HEPES (pH 7.0)]. Three separate experiments for each lipsome formulation were carried out, and the data were fitted separately into a one-site affinity model. The energy of dilution was measured by injecting the liposome formulation into 4 mM HEPES (pH 7.0).

Circular Dichroism Experiments. Circular dichroism (CD) experiments were performed using a JASCO J-715 spectropolarimeter (Beckmann-Coulter) at 20 °C. CD spectra of pDNA were recorded between 220 and 350 nm using a step resolution of 0.2 nm, a scan speed of 10 nm/min, a bandwidth of 1 nm, and a sensitivity of 10 mdeg. All measurements were carried out in duplicate and averaged to one single curve. pDNA exhibits a maximum CD amplitude at 273 nm, which was used for time experiments. In these, the CD of 24 nM pDNA [4 mM HEPES (pH 7.0)] at 273 nm was measured for 5 min before addition of liposomes (50 μL, 0.3 mM) while the sample was in the spectrophotometer, mixed by bubbling air through the sample (2−3 s), and the CD amplitude at 273 nm was followed over the course of 60 min.

Photon Correlation Spectroscopy. At the end of each titration experiment (ITC), 10 μL of the ITC end titration emulsion was diluted with 190 μL of HEPES buffer (pH 7, 4 mM), and particle sizes were measured on an N4 plus MD submicron particle analyzer (Beckman Coulter, High Wycombe, Buckinghamshire, U.K.). All measurements were performed at 20 °C and recorded at 90 °C, with an equilibration time of 1 min and individual run times of 300 s. The refractive index of the buffer was set to 1.333. Unimodal analysis was used throughout to calculate the mean particle size and standard distribution in four separate experiments.

Turbidity Assay. LD (60 μL) at 100 μg/mL (pDNA) was mixed with 240 μL of FCS, and the mixture was incubated at 37 °C during gentle shaking. Dynamic changes in the turbidity of LD(DC-Chol) and LD(CDAN) after exposure to serum were monitored at 600 nm on an Ultrospec 4000 UV−VIS photospectrometer (Pharmacia) at the indicated times.

Transfection Experiments. HeLa and Panc-1 cells were grown in 48-well plates until the cells were semiconfluent (∼10^5 cells) in 500 μL of normal growth medium (DMEM complemented with 10% fetal calf serum). Transfection procedures were carried out using 0.5 μg of pDNA per well with incubation times of 30 and 150 min, respectively.

For transfections in OptiMEM, DMEM (50 and 100% serum), the growth medium was removed and the cells were washed with PBS prior to addition of transfection medium followed by the addition of the samples. LipofectAMINE™ transfections were carried out according to the manufacturer's optimized procedures. After the respective transfection times, the medium was removed and replaced with normal growth medium and the cells were left for 24 h before being lysed and assayed for β-galactosidase activity by luminescence. Protein concentrations were determined by the BCA assay (Pierce, Rockford, IL).

RESULTS

Isothermal Titration Calorimetry (ITC) with CDAN/DOPE Liposomes. A fixed concentration of pDNA (18.1 or 24.1

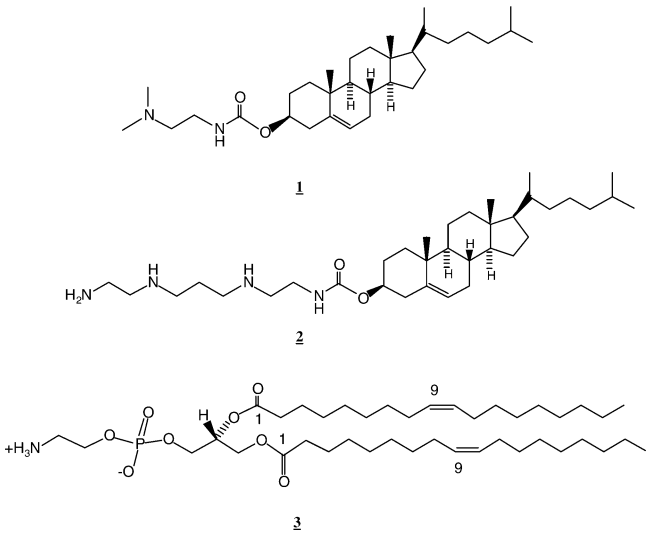

FIGURE 1: Chemical structures of the lipids investigated as part of liposomes in this study: (**1**) DC-Chol, (**2**) CDAN, and (**3**) neutral helper lipid DOPE.

nM) was titrated with liposomes (25 injections of 10 μL each) of a 3.84 or 1.92 mM solution in 4 mM HEPES (pH 7.0), yielding a mainly triphasic output (Figure 2A). An initial exothermic phase (a) was followed by a set of endothermic signals (b) succeeded by an exothermic dilution of excess liposomes into buffer (c). Phase (a) was attributed to the complexation of pDNA with cationic liposomes to form LD particles. Interruption of the titration process during the exothermic phase showed that no aggregation was visible at this stage of the titration. In phase (b), aggregation was observed, which is manifested as endothermic signals. Phase (c) is the exothermic dilution of excess cationic liposomes into buffer as determined by a separate titration experiment injecting liposomes into buffer (Figure 3). Intriguingly, phase (a) was itself found to be biphasic upon closer inspection (Figure 2B).

A control experiment was then performed in which cationic liposomes were injected into buffer in the absence of pDNA, revealing strong exothermic signals due to the dilution of concentrated cationic liposomes (Figure 3). An overlay of the previous pDNA data and this control data set strongly suggested that cationic liposome dilution effects could account for the first phase of phase (a) [Figure 2B, (a)], while the second phase [Figure 2B, (b)] could be attributed to actual cationic liposome−pDNA interactions. As a result, only these second phase signals were integrated for the subsequent fitting of binding data to a single-affinity binding model. Since this first exothermic phase (a) is a regime with a low overall positive/negative charge ratio and no aggregation was observed, fitting of these data to a single-site binding model allowed for the determination of the thermodynamic values of the binding event. Naturally, this procedure limits the accuracy of the thermodynamic profile obtained from the curve fittings. However, by varying the concentrations of both pDNA (24.1 or 18 nM) and liposomes (lipid concentration, 1.92 or 3.84 mM) in separate titration experiments, we achieved an overall estimation of the best fit to a single-affinity binding site model.

From these fittings, an average value of 6500 ± 500 lipids per plasmid DNA (*m*/*m*) was obtained, which gives an overall K_d value of 19 ± 3 μM. Other thermodynamic values are

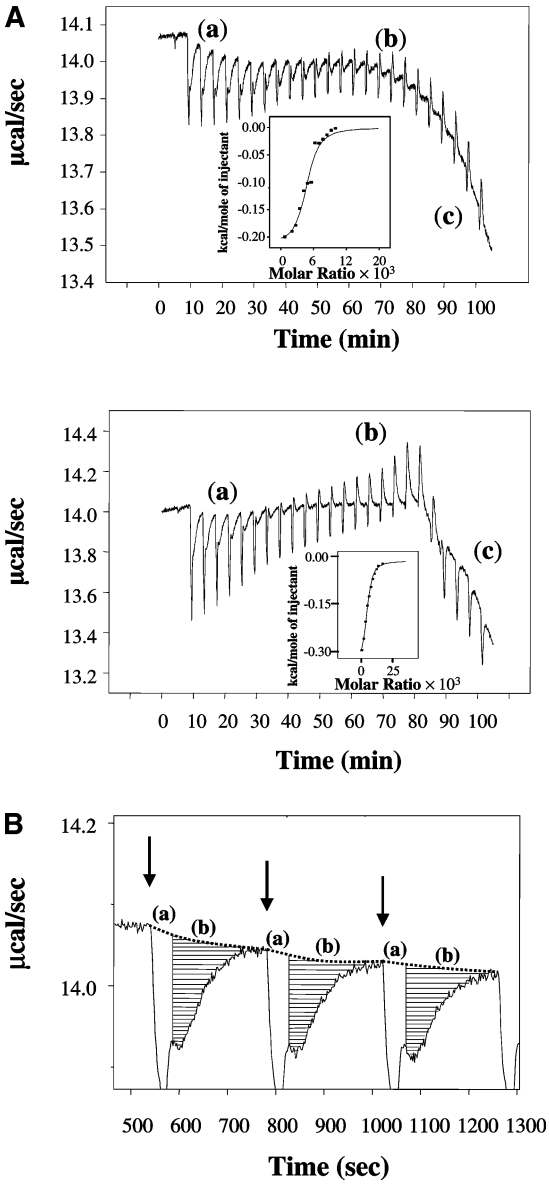

FIGURE 2: (A) Representative ITC data obtained from the injection of CDAN/DOPE (50:50, *m*/*m*) liposomes into pDNA: (top) 24 injections (12 μL each) of liposomes (1.92 mM) into pDNA (24.1 nM) and (bottom) 24 injections (12 μL each) of liposomes (3.84 mM) into pDNA (24.1 nM) and (a) exothermic binding region, (b) endothermic signals from pDNA condensation and aggregation, and (c) exothermic profile of excess liposome dilution into buffer. The respective curve fittings to a one-site affinity model are depicted as insets at the bottom right. (B) Biphasic nature of exothermic signals observed when titrating CDAN/DOPE (50:50, *m*/*m*) liposomes into pDNA (cf. Figure 2A): (a) exothermic dilution/rehydration of liposome in buffer and (b) exothermic signal of pDNA complexation by liposomes. Note that only the second (hatched) part of the signal was integrated for the extraction of thermodynamic parameters.

given in Table 1. Most notably, cationic liposome−DNA interactions occurred with increasing system entropy (6.2 ± 0.2 cal/mol) and a decrease in the enthalpy of binding ($\Delta H°$) of −0.5 kcal/mol.

Isothermal Titration Calorimetry (ITC) with DC-Chol/DOPE Liposomes. ITC titrations were carried out as described above by titrating cationic liposomes against a fixed concentration of pDNA (18 or 24.1 nM) (Figure 4).

In this case, the titration output was only biphasic with an initial exothermic phase (a) followed by an endothermic

Table 1: Thermodynamic Parameters for Binding of Two Cationic Liposome Formulations, DC-Chol/DOPE (60:40, *m*/*m*) and CDAN/DOPE (50:50, *m*/*m*), to pDNA

liposome	K_d (μM)[a]	*N* for lipid−pDNA (m/m)[a]	$\Delta H°$ (kcal/mol)[a]	$T\Delta S°$ (kcal/mol)[b]	size (nm)[c]
CDAN/DOPE[d] (50:50, *m*/*m*)	19 ± 3	6500 ± 500	−0.5 ± 0.1	6.2 ± 0.3	222 ± 25
DC-Chol/DOPE (60:40, *m*/*m*)	2 ± 0.5	27000 ± 1000	−1.7 ± 0.1	6 ± 0.3	261 ± 50

[a] Measured by isothermal titration calorimetry at 298 K. [b] Obtained from the relationship $\Delta G° = \Delta H° - T\Delta S°$ for a *T* of 298 K. [c] Determined by dynamic light scattering (PCS) of a sample taken at the end of the ITC titration experiment. [d] CDAN/DOPE (50:50, *m*/*m*) is commercially known as Trojene™.

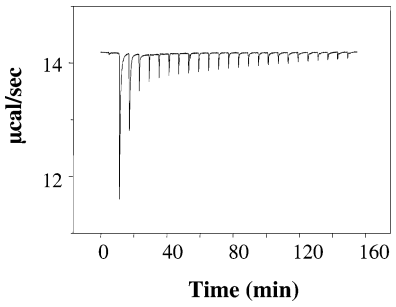

FIGURE 3: Profile of dilution of CDAN/DOPE (50:50, *m*/*m*) liposomes (1.92 mM, 24 injections of 12 μL each) in 4 mM HEPES (pH 7.0).

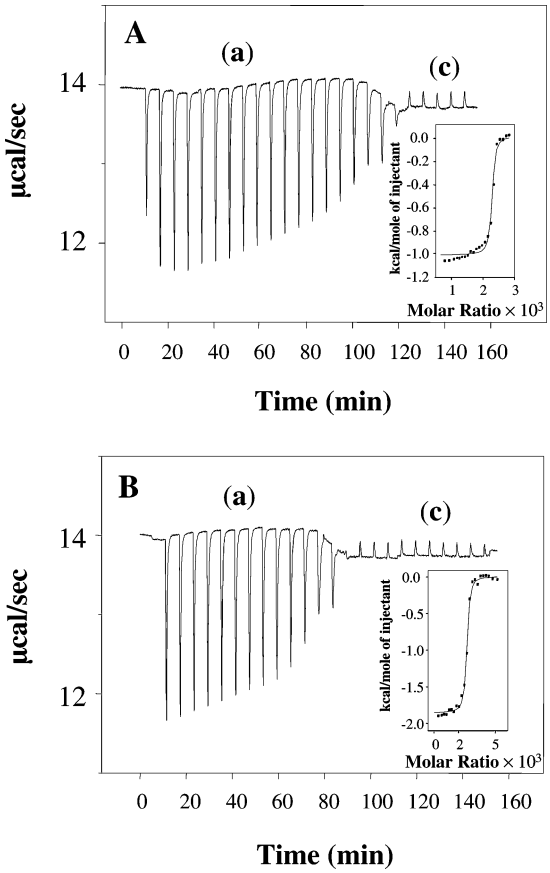

FIGURE 4: Representative ITC data obtained from the injection of DC-Chol/DOPE (60:40, *m*/*m*) liposomes into pDNA (A) 24 injections (12 μL each) of liposomes (4.16 mM) into pDNA (24.1 nM) and (B) 24 injections (12 μL each) of liposomes (4.16 mM) into pDNA (18.1 nM) and (a) exothermic binding region and (c) exothermic profile of excess liposome dilution into buffer. The respective curve fittings into a one-site affinity model are depicted as insets at the bottom right.

phase (b). Phase (a) was attributed once again to the complexation of pDNA with cationic liposomes to form LD particles and phase (c) to higher-order particle formation/

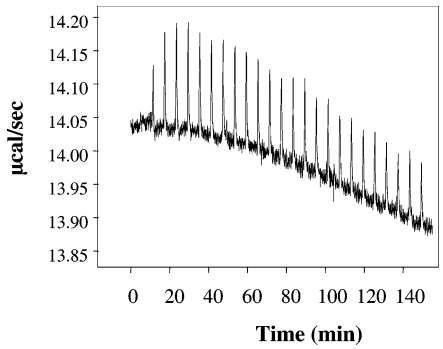

FIGURE 5: Profile of dilution of DC-Chol/DOPE (60:40, *m*/*m*) liposomes (4.16 mM, 24 injections of 12 μL each) in 4 mM HEPES (pH 7.0).

particle aggregation and/or cationic liposome dilution. Intriguingly, a third dilution phase was not observed, and phase (a) did not show any obvious biphasic characteristics. In point of fact, DC-Chol/DOPE dilution into buffer was found to be mildly endothermic (Figure 5), in complete contrast to CDAN/DOPE dilution. Furthermore, no heavy aggregation was observed as with CDAN/DOPE liposomes.

Therefore, complete data corresponding with phase (a) were fit as described above, giving an equilibrium dissociation constant, K_d, of 2 ± 0.5 μM, suggesting that interactions of DC-Chol/DOPE liposomes with pDNA were 1 order of magnitude stronger than those of CDAN/DOPE liposomes with an average value of 27 000 ± 1000 lipids/pDNA, 4-fold greater than that observed with CDAN/DOPE liposomes. Other thermodynamic data are given in Table 1. The increase in system entropy was in the same range as for the CDAN/DOPE system.

Circular Dichroism (CD) Spectroscopy. Double-stranded pDNA has a characteristic positive CD signal at 273 nm, ΔOD_{273}, that is derived from n−π* electronic transitions of adenine bases (*29*). The plasmid DNA used for this study was estimated by gel electrophoresis analysis to be dominantly supercoiled (*30*). Signal intensity has been observed to decrease gradually with binding of a cationic species such as the adenoviral core peptide μ (mu) (*30*) or other cationic species (*31*). When the CD spectrum of a sample of pDNA [24 nM in 4 mM HEPES (pH 7.0)] was monitored as a function of time (60 min), ΔOD_{273} (0.000085) was found to be steady. After the addition of CDAN/DOPE liposomes (50 μL, 0.3 mM) to 300 μL of pDNA (24 nM), the value of ΔOD_{273} was found to change continuously over the period of monitoring (60 min) (Figure 6). Initially, the value of ΔOD_{273} fluctuated over a period of 25−30 min. Thereafter, the value of ΔOD_{273} increased to an intermediate plateau value over a period of 30 min. In contrast, after the addition of DC-Chol/DOPE liposomes to pDNA (24 nM), the value of ΔOD_{273} remained constant after the initial accommodation (Figure 6). These data were interpreted as suggesting that

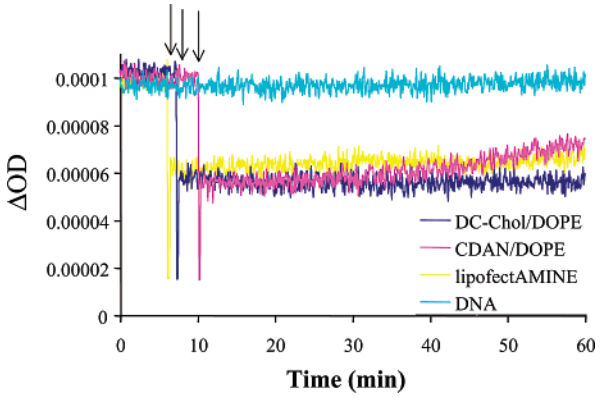

FIGURE 6: Circular dichroism of the maximum CD amplitude of pDNA (0.12 mg/mL, 200 μL) at 273 nm (light blue). The CD amplitude of pDNA observed for 60 min at 293 K after addition of liposomes (arrows) in a total volume of 100 μL of HEPES (4 mM, pH 7.0), which also results in a decrease in the ΔOD due to dilution. For each experiment, the overall charge ratio of pDNA to lipid was 2: (light blue) CDAN/DOPE (1.5 μL of a 4.5 mg/mL solution), (dark blue) DC-Chol/DOPE (5 μL of a 4.5 mg/mL solution), and (pink) LipofectAMINE (3 μL of a 2 mg/mL solution). Note that CDAN lipoplexes exhibit substantial dynamics over at least 60 min compared to all other lipoplexes.

DC-Chol/DOPE liposomes were forming relatively stable LD particles with pDNA while CDAN/DOPE liposomes were forming metastable LD particles that underwent further structural adjustments after the initial period of LD particle formation.

Photon Correlation Spectroscopy. Dynamic light scattering is a reliable method for estimating particle sizes within the scope of 3−3000 nm. After completion of each ITC experiment, a sample of 10 μL was diluted with 190 μL of HEPES and subjected to a size analysis (Table 1). LD particles from DC-Chol/DOPE liposomes exhibited less heavy aggregation than LD derived from CDAN/DOPE liposomes. By dilution in HEPES (20-fold), the aggregation was dissolved readily. Size analysis revealed that CDAN/DOPE and DC-Chol/DOPE LD particles were on the order of 222 ± 25 and 261 ± 50 nm in diameter, respectively, in line with our previous observations of LD particles by cryoelectron microscopy (*5*, *22*). However, the actual size variation was apparently greater than these error limits suggested as indicated by polydispersity indeces of ∼0.3. This may be due to the fact that LD mixtures were prepared in this case by adding aliquots of cationic liposomes to a solution containing pDNA rather than the reverse. In general, the addition of aliquots of pDNA to a solution of cationic liposomes appeared to give more reproducible LD particle formation than the reverse (*4*, *6*).

Turbidity Assays. LD particles have the tendency to aggregate even in a low-ionic strength solution. This feature is dramatically enhanced in the presence of serum. Therefore, the aggregation properties of LD mixtures prepared from CDAN/DOPE and DC-Chol/DOPE cationic liposomes were compared as a function of time in the presence of 0, 10, and 60% serum by means of turbidity assays (*5*, *22*). The absorbance at 600 nm, A_{600}, was observed as a function of time following the combination of each LD mixture with buffer containing the appropriate level of fetal calf serum (FCS). Neither LD mixture showed signs of aggregation activity over a period of 3 h at 37 °C in 0 or 10% serum, but CDAN/DOPE LD mixtures were observed to be considerably more aggregation prone than DC-Chol/DOPE LD mixtures in the presence of 60% serum as evidenced by the rapid increase in turbidity after incubation for 100 min at 37 °C in the former compared with the latter case (Figure 7). Such an enhanced tendency toward aggregation is consistent with the observed metastability of CDAN/DOPE LD particles in comparison with DC-Chol/DOPE LD particles (see above).

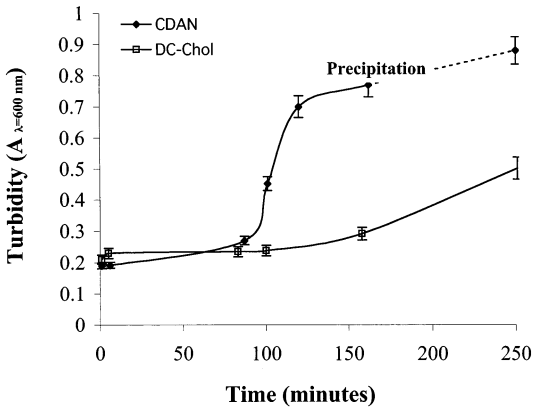

FIGURE 7: Turbidity assays monitoring the growth of LD(DC-Chol) and LD(CDAN) particles after incubation with fetal calf serum (FCS).

Transfection Experiments. Barenholz et al. showed that not the pDNA structure but phase instability and maximum heterogeneity of lipoplexes contribute to optimal transfection efficiency (*32*). As a result, we did not investigate the impact of different pDNA structures on transfection levels. LD transfections were performed with two dividing cell lines, HeLa and Panc-1 cells, under different experimental conditions. Transfections were performed in so-called optimized transfection medium (OptiMEM) and in normal growth medium containing either 10 or 50% serum. Transfections were also studied in medium containing up to 100% serum as well. CDAN/DOPE liposome-mediated transfection was particularly effective in normal growth medium but less so in OptiMEM and much less so in the presence of very high serum levels. This was true irrespective of whether short (30 min) or long (150 min) transfection times were utilized (Figure 8). In comparison, CDAN/DOPE liposome-mediated transfections were significantly more efficient than DC-Chol/DOPE liposome-mediated transfections, in line with our previous observations (*5*, *22*), and without a clear preference for one transfection medium over another (Figure 8). Furthermore, CDAN/DOPE liposome-mediated transfections were found to be equivalent to if not more effective in performance than all those selected for comparison.

DISCUSSION

The relationship between cytofectin structures, LD properties, and transfection efficiency *in vitro* and/or *in vivo* has proven to be difficult to determine in all but a small handful of cases (*5*, *22*). Previously, we suggested that efficient transfection *in vitro* mediated by cationic liposomes formulated from DC-Chol and DC-Chol polyamine analogues was a function of two main characteristics: (1) a weakened capacity to bind, charge neutralize, and condense pDNA and (2) the presence of amine functional groups with pK_a values perturbed to values of approximately ≤7 (*5*). Both characteristics appeared to synergise to promote efficient transfec-

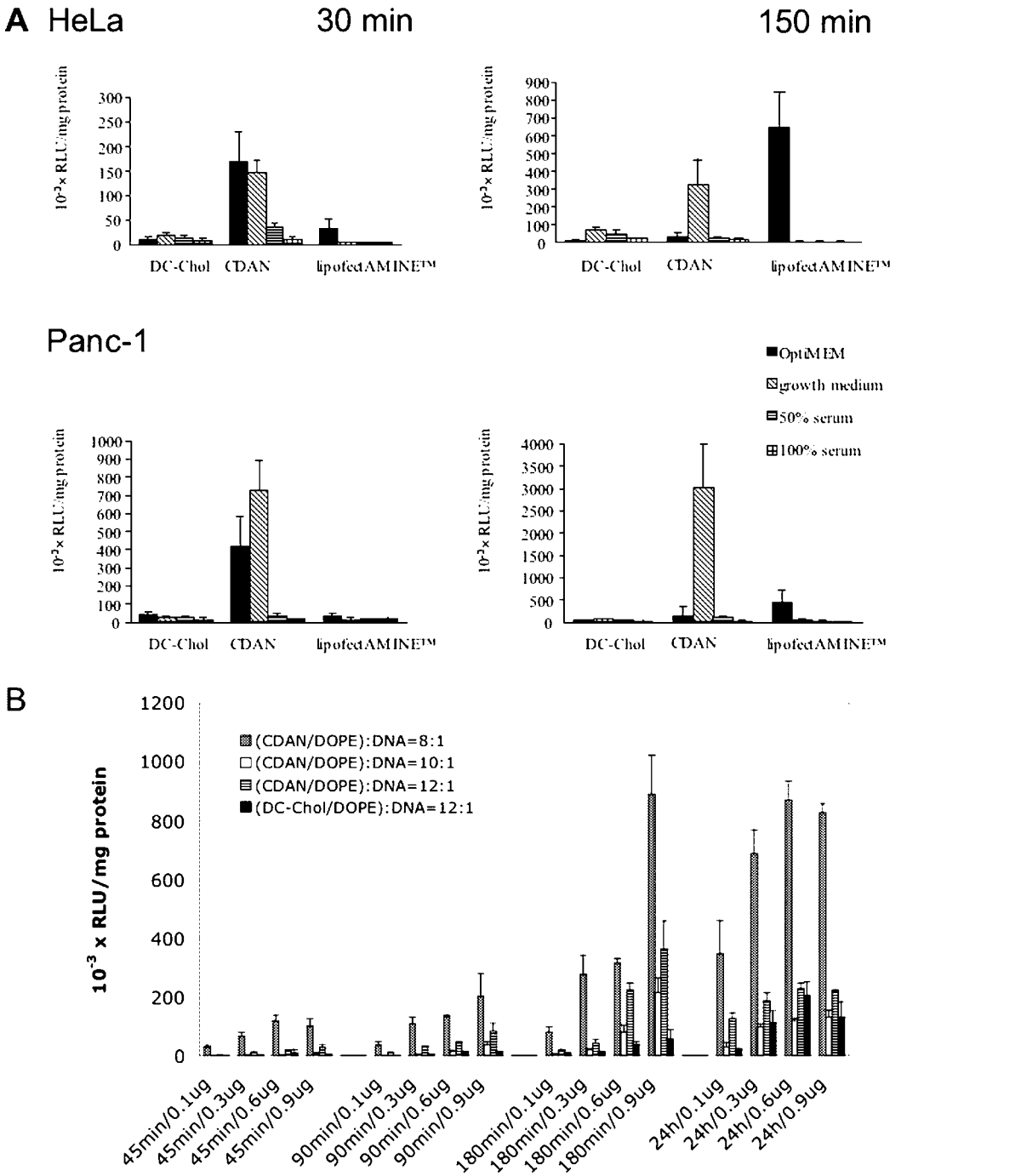

FIGURE 8: Transfection experiments with HeLa and Panc-1 cells. (A) The panels on the left show the level of expression of β-galactosidase per milligram of protein for 30 min transfection times, whereas the panels on the right represent the situation of 150 min transfection times in HeLA (top) and Panc-1 (bottom) cells: (black bars) OptiMEM, (gray bars, diagonally hatched) DMEM (10% serum), (dark gray bars, horizontally hatched) DMEM (50% serum), and (cubic hatched bars) 100% serum. DC-Chol/DOPE (60:40, *m*/*m*) and CDAN/DOPE (50:50, *m*/*m*; Trojene™) lipoplexes were each time compared with lipofectAMINE™. All experiments were carried out in quadruplicate. (B) Time course experiment investigating the impact of different quantities of lipoplex (micrograms of pDNA) for different incubation times of lipoplexes with Panc-1 cells.

tion *in vitro*. Using a combination of isothermal titration calorimetry (ITC) (Figures 2−5 and Table 1), circular dichroism (CD) (Figure 6) and photon correlation spectroscopy (PCS) (Table 1), and turbidity assays (Figure 7), we have revisited the physical properties of LD particles formulated from pDNA (7528 bp) and either CDAN/DOPE (50:50, *m*/*m*) or DC-Chol/DOPE (60:40, *m*/*m*) cationic liposomes. Although data are difficult to extract due to multiphase binding events between liposomes and DNA, ITC data clearly demonstrate that LD particles prepared from CDAN/DOPE liposomes comprise lipid−pDNA interactions that are weaker than those measured in DC-Chol/DOPE liposomes (Table 1). At saturation, the number of CDAN or DC-Chol molecules per pDNA molecule is 3250 or 16 200, respectively. Therefore, given the determined K_d values, the microscopic dissociation constants per cytofectin, κ_d, are 62 and 32 mM, respectively. Furthermore, CD data show that CDAN/DOPE liposome-derived LD particles are structurally plastic (metastable) following LD particle formation, while DC-Chol/DOPE liposome-derived LD particles are not.

The origins of both differences may rest with the structures of the relevant cytofectins. Each DC-Chol possesses a single tertiary amine ($pK_a = 7.8$) and CDAN two secondary and one primary amine with measured pK_a values of 9.3 ± 0.01, 7.6 ± 0.01, and 5.7 ± 0.01, giving a net charge of 1.6−1.8 at pH 7 (*5*). Accordingly, dilution effects involving CDAN/DOPE cationic liposomes might be expected to be more substantial than effects of DC-Chol/DOPE cationic liposomes. CDAN has a higher charge than each DC-Chol and has the capacity to support both exothermic hydrogen bonding with water as well as dynamic protonation equilibria. Furthermore, the persistence of free, unprotonated amine functional groups at pH 7 may aid in explaining the structural plasticity of CDAN/DOPE liposome-derived LD particles. After cationic liposome dilution and complexation with pDNA over the course of 30 min, LD particles are generated, but the presence of pDNA in close association with positively charged CDAN/DOPE liposomes could act to perturb lower amine pK_a values upward, encouraging further amine functional group protonation (*5*). Subsequent slow (time scale of more than minutes) structural adjustment and/or rearrangements of LD particles in response to such an additional protonation could then explain the observed structural plasticity of CDAN/DOPE liposome-derived LD particles (Figure 6). Finally, the highly interactive character of the CDAN headgroup with water (Figure 3) in comparison with the DC-Chol headgroup (Figure 5) could certainly offer an explanation for the higher affinity of DC-Chol/DOPE cationic liposomes for pDNA in comparison with that of CDAN/DOPE cationic liposomes. Ordered hydration cages more extensive in the case of the CDAN polyamine side chain than in the case of DC-Chol would certainly need to be disrupted for efficient charge−charge interactions with pDNA to take place. This could contribute to a weakening of CDAN/DOPE liposome−pDNA interactions in comparison with DC-Chol/DOPE liposome−pDNA interactions (*33*−*36*).

Bloomfield and co-workers (*37*) and we (*21*, *30*) have previously demonstrated that low-molecular mass molecules such as cobalt hexamine, spermidine, or the cationic peptides such as μ (mu) (from the adenovirus core) and protamine (from salmon sperm) trigger pDNA condensation when 67−80% of phosphodiester backbone negative charges have been neutralized. An electrostatic two-stage mechanism put forth by Bloomfield and co-workers accounts for the majority of the energies measured for the interactions between small positively charged counterions and the pDNA phosphodiester backbone (*37*). pDNA condensation is subsequently driven by hydrophobic interactions, interactions that are even more significant where cationic liposome-mediated pDNA condensation is involved given the hydrophobic character of the liposome bilayer.

Cationic liposome-mediated pDNA condensation is made even more complex due to the substantial size (90 ± 15 nm) and the highly positive surface charge of the condensing particle. Some liposome formulations have been shown to exhibit cooperative DNA binding, which makes the process even more complicated to analyze (*38*). Furthermore, changes in the pK_a of amine functionalities of the lipids due to changes in the microenvironment after complexation contribute to an already complex binding event. Studies performed by Lobo et al. (*39*) have demonstrated that in addition to the electrostatically or entropically driven binding, reprotonation of the DOPE component in both DOTAP/DOPE and DDAB/DOPE liposomes due to a pK_a change played an important part in binding. Accordingly, cationic liposome-mediated pDNA condensation requires control of the order and rate of mixing of cationic liposomes and pDNA for proper control of the homogeneity of LD particle formation (*6*, *40*, *41*).

As a consequence of all of the above, a third component such as a cationic peptide has been used to partially neutralize and condense pDNA prior to subsequent complexation with cationic liposomes. Such a ternary LD approach has been shown by us, and others, to significantly enhance the ease and reproducibility of pDNA formulation into a synthetic gene delivery system (*20*, *30*, *42*−*44*).

Despite such formulation problems, simple binary LD systems are still valuable tools for the transfection of cell lines *in vitro* and may yet have applications to *ex vivo* and *in vivo* gene therapy or DNA vaccines (*45*) with further improvements in understanding. For this reason, CDAN/DOPE cationic liposome-mediated transfections of cells were studied alongside transfections mediated by DC-Chol/DOPE cationic liposomes and other well-known commercially available cationic liposome/micelle agents (Figure 8). The CDAN/DOPE cationic liposome-mediated process *in vitro* was clearly superior to the DC-Chol/DOPE liposome-mediated process under all the conditions that were tested. In light of the conclusions drawn from previous biophysical comparisons (*5*, *22*) and the results discussed above, we suggest two modified reasons for this. First, the fact that CDAN/DOPE liposome−pDNA interactions are weaker than DC-Chol/DOPE liposome−pDNA interactions may still be important. However, more significant may be the presence of amine functional groups with pK_a values perturbed to values of approximately ≤ 7. As discussed previously (*5*, *22*), such functional groups may have not only the capacity to buffer endosome compartments following the entry of LD particles into cells thereby facilitating endosomolysis and the escape of pDNA into the cytosol but also may be a significant cause of LD particle plasticity, as described above.

Structural plasticity could have two consequences. First, CDAN/DOPE−pDNA LD particles have a greater tendency to microaggregate in transfection media than DC-Chol/DOPE−pDNA LD particles. As a result, they tend to create larger particles with a potentially greater capacity to sediment upon and coat the surface of cells in transfection wells, hence facilitating the transport of pDNA into these cells. Such a suggestion is in line with the conclusions of others concerning the importance of larger LD particles for efficient *in vitro* transfection (*46*). As a matter of fact, non-extruded Trojene™ yields dramatically increased transfection levels compared to the levels of the extruded form used in this study. Second, CDAN/DOPE−pDNA LD particles may have a greater tendency to interact with and accommodate serum proteins on their surfaces. Under controlled circumstances, this is known to provide a nonspecific boost to transfection by facilitating endosomolysis and consequent pDNA escape into the cytosol (*47*, *48*). The turbidity data described here support the idea that CDAN/DOPE−pDNA LD particles may be more interactive with negatively charged serum components, including proteins, than DC-Chol/DOPE−pDNA LD particles (Figure 7). Assuming that all amine functional groups

are protonated and interacting with pDNA phosphodiester backbone, under these conditions CDAN/DOPE−pDNA LD particles would therefore have an overall positive-to-negative charge ratio (*N*/*P*) of 0.64 and DC-Chol/DOPE−pDNA LD particles an *N*/*P* ratio of 1.08 at equilibrium. As a result, excess cytofectin is applied to render the overall charge of the particles positive, which is a prerequisite for the effective transfection of cells.

In conclusion, this thermodynamic and biophysical analysis of DNA complexation and condensation with the two cationic liposome systems (CDAN/DOPE and DC-Chol/DOPE, respectively) demonstrates that the two cationic liposome formulations exhibit a distinct individual thermodynamic profile of lipoplex formation. Both liposome formulations are driven by large enthalpic and entropic contributions from the cationic amphiphiles. The metastability of CDAN/DOPE lipoplexes may be ascribed to changes in the lowest pK_a value of one of the three amines after complexation with DNA. Because of this metastability and the increased positive charge, CDAN/DOPE lipoplexes exhibit a stronger tendency to form large aggregates, which is not the case for DC-Chol/DOPE lipoplexes. Such a tendency to form large and heterogeneous aggregates may have a positive influence on the transfection efficacy *in vitro*, but is, of course, highly problematic *in vivo*. Evidence from *in vivo* experiments suggests that serum interactions substantially destabilize LD systems and prevent efficient transfection from taking place (*26*, *41*, *49*−*51*). The substantial perturbation of the maximal CD signal of pDNA when complexed with CDAN/DOPE liposomes suggests that these lipoplexes are highly dynamic species and that for at least an initial period of 1 h, substantial rearrangements of the lipoplex structure take place. Successful drug and gene delivery systems rely heavily on stable, well-defined, and reproducible liposome formulations. This basic study into the thermodynamics and dynamic behavior of lipoplex formation and interactions should contribute to a better understanding of lipoplexes and hence for the design and characterization of novel gene delivery systems for use as synthetic gene and drug delivery vehicles.

REFERENCES

1. Miller, A. D. (1998) *Angew. Chem., Int. Ed. 37*, 1769−1785.
2. Lander, E. S., Linton, L. M., Birren, B., Nusbaum, C., Zody, M. C., et al. (2001) *Nature 409*, 860−921.
3. Venter, J. C., Adams, M. D., Myers, E. W., Li, P. W., Mural, R. J., et al. (2001) *Science 291*, 1304−1320.
4. Cooper, R. G., Etheridge, C. J., Stewart, L., Marshall, J., Rudginsky, S., et al. (1998) *Chem. Eur. J. 4*, 137−151.
5. Geall, A. J., Taylor, R. J., Earll, M. E., Eaton, M. A. W., and Blagbrough, I. S. (2000) *Bioconjugate Chem. 11*, 314−326.
6. Zelphati, O., Nguyen, C., Ferrari, M., Felgner, J., Tsai, Y., et al. (1998) *Gene Ther. 5*, 1272−1282.
7. Pector, V., Backmann, J., Maes, D., Vandenbranden, M., and Ruysschaert, J. M. (2000) *J. Biol. Chem. 275*, 29533−29538.
8. Templeton, N. S., Lasic, D. D., Frederik, P. M., Strey, H. H., Roberts, D. D., et al. (1997) *Nat. Biotechnol. 15*, 647−652.
9. Alton, E., Middleton, P. G., Caplen, N. J., Smith, S. N., Steel, D. M., et al. (1993) *Nat. Genet. 5*, 135−142.
10. Harbottle, R., Cooper, R., Miller, A., Williamson, B., Coutelle, C., et al. (1995) *J. Cell. Biochem.*, 394.
11. Colin, M., Harbottle, R. P., Knight, A., Kornprobst, M., Cooper, R. G., et al. (1998) *Gene Ther. 5*, 1488−1498.
12. Fife, K., Bower, M., Cooper, R. G., Stewart, L., Etheridge, C. J., et al. (1998) *Gene Ther. 5*, 614−620.
13. Themis, M., Forbes, S. J., Chan, L., Cooper, R. G., Etheridge, C. J., et al. (1998) *Gene Ther. 5*, 1180−1186.
14. Cooper, R. G., Harbottle, R. P., Schneider, H., Coutelle, C., and Miller, A. D. (1999) *Angew. Chem., Int. Ed. 38*, 1949−1952.
15. Colin, M., Maurice, M., Trugnan, G., Kornprobst, M., Harbottle, R. P., et al. (2000) *Gene Ther. 7*, 139−152.
16. Fellowes, R., Etheridge, C. J., Coade, S., Cooper, R. G., Stewart, L., et al. (2000) *Gene Ther. 7*, 967−977.
17. Jost, P. J., Harbottle, R. P., Knight, A., Miller, A. D., Coutelle, C., et al. (2001) *FEBS Lett. 489*, 263−269.
18. Miller, N., and Vile, R. (1995) *FASEB J. 9*, 190−199.
19. Murray, K. D., McQuillin, A., Stewart, L., Etheridge, C. J., Cooper, R. G., et al. (1999) *Gene Ther. 6*, 190−197.
20. Murray, K. D., Etheridge, C. J., Shah, S. I., Matthews, D. A., Russell, W., et al. (2001) *Gene Ther. 8*, 453−460.
21. Colin, M., Moritz, S., Fontanges, P., Kornprobst, M., Delouis, C., et al. (2001) *Gene Ther. 8*, 1643−1653.
22. Stewart, L., Manvell, M., Hillery, E., Etheridge, C. J., Cooper, R. G., et al. (2001) *J. Chem. Soc., Perkin Trans. 2*, 624−632.
23. Moritz, S., Colin, M., Keller, M., Klonjkowski, B., Capeau, J., et al. (2003) *Arch. Virol. 148*, 1−18.
24. Tagawa, T., Manvell, M., Brown, N., Keller, M., Perouzel, E., et al. (2002) *Gene Ther. 9*, 564−576.
25. Keller, M., Harbottle, R. P., Perouzel, E., Morvane, C., Imran, S., et al. (2003) *ChemBioChem 4*, 286−298.
26. Li, S., Tseng, W. C., Stolz, D. B., Wu, S. P., Watkins, S. C., et al. (1999) *Gene Ther. 6*, 585−594.
27. Duffels, A., Green, L. G., Ley, S. V., and Miller, A. D. (2000) *Chem. Eur. J. 6*, 1416−1430.
28. Sambrook, J., Fritsch, E. F., and Maniatis, T. (1989) *Molecular Cloning: A Laboratory Manual*, pp C.1, Cold Spring Harbor Laboratory Press, Plainview, NY.
29. Maestre, M. F., Gray, D. M., and Cook, R. B. (1971) *Biopolymers 10*, 2537−2553.
30. Keller, M., Tagawa, T., Preuss, M., and Miller, A. D. (2002) *Biochemistry 41*, 652−659.
31. Durand, M., Maurizot, J.-C., Borazan, H. N., and Hélène, C. (1975) *Biochemistry 14*, 563−570.
32. Simberg, D., Danino, D., Talmon, Y., Minsky, A., Ferrari, M. E., et al. (2001) *J. Biol. Chem. 276*, 47453−47459.
33. Bloomfield, V. A. (1991) *Biopolymers 31*, 1471−1481.
34. Bloomfield, V. A. (1996) *Curr. Opin. Struct. Biol. 6*, 334−341.
35. Bloomfield, V. A., He, S. Q., Li, A. Z., and Arscott, P. B. (1991) *Biochem. Soc. Trans. 19*, 496.
36. Bloomfield, V. A., and Rouzina, I. (1998) *Methods Enzymol. 295*, 364−378.
37. Matulis, D., Rouzina, I., and Bloomfield, V. A. (2000) *J. Mol. Biol. 296*, 1053−1063.
38. Gershon, H., Ghirlando, R., Guttman, S. B., and Minsky, A. (1993) *Biochemistry 32*, 7143−7151.
39. Lobo, B. A., Davis, A., Koe, G., Smith, J. G., and Middaugh, C. R. (2001) *Arch. Biochem. Biophys. 386*, 95−105.
40. Zelphati, O., Uyechi, L. S., Barron, L. G., and Szoka, F. C. (1998) *Biochim. Biophys. Acta 1390*, 119−133.
41. Turek, J., Dubertret, C., Jaslin, G., Antonakis, K., Scherman, D., et al. (2000) *J. Gene Med. 2*, 32−40.
42. Kreiss, P., and Scherman, D. (1999) *Med. Sci. 15*, 669−676.
43. Escriou, V., Ciolina, C., Helbling-Leclerc, A., Wils, P., and Scherman, D. (1998) *Cell Biol. Toxicol. 14*, 95−104.
44. Kreiss, P., Cameron, B., Rangara, R., Mailhe, P., Aguerre-Charriol, O., et al. (1999) *Nucleic Acids Res. 27*, 3792−3798.
45. Johnston, S. A., Talaat, A. M., and McGuire, M. J. (2002) *Arch. Med. Res. 33*, 325−329.
46. Ross, P. C., and Hui, S. W. (1999) *Gene Ther. 6*, 651−659.
47. da Cruz, M. T. G., Simoes, S., Pires, P. P. C., Nir, S., and de Lima, M. C. P. (2001) *Biochim. Biophys. Acta 1510*, 136−151.
48. Simoes, S., Slepushkin, V., Duzgunes, N., and de Lima, M. C. P. (2001) *Biochim. Biophys. Acta 1515*, 23−27.
49. de Ilarduya, C. T., and Duzgunes, N. (2000) *Biochim. Biophys. Acta 1463*, 333−342.
50. Vitiello, L., Bockhold, K., Joshi, P. B., and Worton, R. G. (1998) *Gene Ther. 5*, 1306−1313.
51. Yi, S. W., Yune, T. Y., Kim, T. W., Chung, H., Choi, Y. W., et al. (2000) *Pharm. Res. 17*, 314−320.

BI0274219